

is not expected, since different genes are thought to have different numbers of copies.

Received May 23; revised July 10, 1973.

- <sup>1</sup> Callan, H. G., *J. Cell Sci.*, **2**, 1 (1967).
- <sup>2</sup> Brown, D. D., Wensink, P. C., and Jordan, E., *J. molec. Biol.*, **63**, 57 (1972).
- <sup>3</sup> Gilbert, W., and Dressler, D., *Cold Spring Harb. Symp. quant. Biol.*, **33**, 473 (1969).
- <sup>4</sup> Buongiorno-Nardelli, M., Arnaldi, F., and Lava-Sanchez, P. A., *Nature new Biol.*, **238**, 134 (1972).
- <sup>5</sup> Arnaldi, F., Lava-Sanchez, P. A., and Buongiorno-Nardelli, M., *Nature*, **242**, 615 (1973).
- <sup>6</sup> Tartof, K. D., *Genetics*, **73**, 57 (1973).
- <sup>7</sup> Ritossa, F. M., Atwood, K. C., and Spiegelman, S., *Genetics*, **54**, 819 (1966).
- <sup>8</sup> Ritossa, F. M., *Proc. natn. Acad. Sci. U.S.A.*, **60**, 509 (1968).
- <sup>9</sup> Atwood, K. C., *Genetics*, **61**, suppl., 319 (1969).
- <sup>10</sup> Keyl, H.-G., *Chromosoma*, **17**, 139 (1965).
- <sup>11</sup> Miller, L., and Knowland, J. S., *J. molec. Biol.*, **53**, 329 (1970).
- <sup>12</sup> Knowland, J. S., and Miller, L., *J. molec. Biol.*, **53**, 321 (1970).
- <sup>13</sup> Hotta, Y., and Stern, H., *J. molec. Biol.*, **55**, 337 (1971).
- <sup>14</sup> Howell, S. H., and Stern, H., *J. molec. Biol.*, **55**, 357 (1971).
- <sup>15</sup> Mirsky, A. E., and Ris, H., *J. gen. Physiol.*, **34**, 451 (1951).
- <sup>16</sup> Calef, E., *Heredity*, **11**, 265 (1957).
- <sup>17</sup> Putriment, A., *Molec. gen. Genet.*, **100**, 321 (1967).
- <sup>18</sup> Murray, N. E., *Genet. Res.*, **15**, 109 (1970).
- <sup>19</sup> Campbell, A. M., *Adv. Genet.*, **11**, 101 (1962).
- <sup>20</sup> Whitehouse, H. L. K., *J. Cell Sci.*, **2**, 9 (1967).
- <sup>21</sup> Giles, N. H., *Cold Spring Harb. Symp. quant. Biol.*, **16**, 283 (1952).
- <sup>22</sup> Pritchard, R. H., *Heredity*, **9**, 343 (1955).
- <sup>23</sup> Mitchell, M. B., *Proc. natn. Acad. Sci. U.S.A.*, **41**, 215 (1955).
- <sup>24</sup> Kitani, Y., Olive, L. S., and El-Ani, A. S., *Am. J. Bot.*, **49**, 697 (1962).
- <sup>25</sup> Ballantyne, G. H., and Chovnick, A., *Genet. Res.*, **17**, 139 (1971).
- <sup>26</sup> Chovnick, A., Ballantyne, G. H., and Holm, D. G., *Genetics*, **69**, 179 (1971).
- <sup>27</sup> Carlson, P. S., *Genet. Res.*, **17**, 53 (1971).
- <sup>28</sup> Stadler, D. R., *Proc. natn. Acad. Sci. U.S.A.*, **45**, 1625 (1959).
- <sup>29</sup> Fogel, S., and Hurst, D. D., *Genetics*, **57**, 455 (1967).
- <sup>30</sup> Whitehouse, H. L. K., and Hastings, P. J., *Genet. Res.*, **6**, 27 (1965).
- <sup>31</sup> Murray, N. E., *Genetics*, **61**, 67 (1969).
- <sup>32</sup> Whitehouse, H. L. K., *Biol. Rev.*, **45**, 265 (1970).
- <sup>33</sup> Whitehouse, H. L. K., *Brookhaven Symp. Biol.*, **23**, 293 (1972).
- <sup>34</sup> Ahmad, A. F., Bond, D. J., and Whitehouse, H. L. K., *Genet. Res.*, **19**, 121 (1972).
- <sup>35</sup> Smith, P. A., and King, R. C., *Genetics*, **60**, 335 (1968).
- <sup>36</sup> Smyth, D. R., and Stern, H., *Nature* (in the press).

# Intraplate Earthquakes, Lithospheric Stresses and the Driving Mechanism of Plate Tectonics

LYNN R. SYKES & MARC L. SBAR

Lamont-Doherty Geological Observatory of Columbia University, Palisades, New York 10964

Focal mechanisms of about eighty intraplate earthquakes and other information on *in situ* stress indicate that the interiors of many lithospheric plates are characterised by large horizontal compressive stresses. These stresses seem to be related to the driving mechanism of plate tectonics.

ABOUT 90% of the world's earthquakes occur along the boundaries of lithospheric plates. Focal mechanism solutions of earthquakes have provided a detailed description of the type of faulting and the nature of the displacements for most of the major plate boundaries<sup>1</sup>. Another class of shocks, intraplate earthquakes, are less numerous than those along plate boundaries and have received relatively little study. Consequently, their cause and tectonic settings have not been well understood.

Here we attempt to determine the type of faulting and to infer the state of stress within lithospheric plates on a worldwide scale from analyses of focal mechanisms of about eighty earthquakes, most of which are located well away from plate boundaries. Our principal result is that a large percentage of these shocks, particularly those not located near mid-ocean ridges or behind subduction zones, are characterised by a predominance of thrust faulting. In the few areas of the world for which they are available, other determinations of the

state of stress from overcoring, hydrofracturing and recent crustal movements support our conclusion that large areas in the interiors of many lithospheric plates are characterised by high horizontal compressive stresses. These seem to be uniform in orientation over sizable regions for the few cases where sufficiently dense data are available.

The very existence of earthquakes in the interiors of the plates indicates that the approximation that plates are undeformed except at their edges is not completely correct even though this assumption seems to be a good working hypothesis for many purposes. The intraplate earthquakes discussed in this paper are all of shallow focus and are located in areas where lithospheric plates are horizontal. Here we present evidence which indicates that the most consistent parameter in focal solutions of shallow earthquakes remote from plate boundaries is the orientation of one of the principal stresses. Earthquakes beneath deep-sea trenches, which involve normal faulting, and intermediate and deep shocks<sup>2</sup> are other examples of intraplate events in which the direction of one of the principal stress axes is consistent for various nearby shocks. In contrast, slip vectors, rather than principal stress axes, are consistent for earthquakes along a given plate boundary<sup>3</sup>.

While intraplate earthquakes are not numerous compared with shocks along active plate margins, intraplate shocks as large as magnitude 7 have occurred in several populated areas including parts of central and eastern North America, Europe, Australia and South Africa. Examples of destructive and large intraplate earthquakes include New Madrid, Missouri 1811–12; Charleston, South Carolina 1886; Cape Ann, Massachusetts 1755; Grand Banks 1929; Meckering, Australia 1968, and several large earthquakes in the St Lawrence Valley<sup>4</sup>.

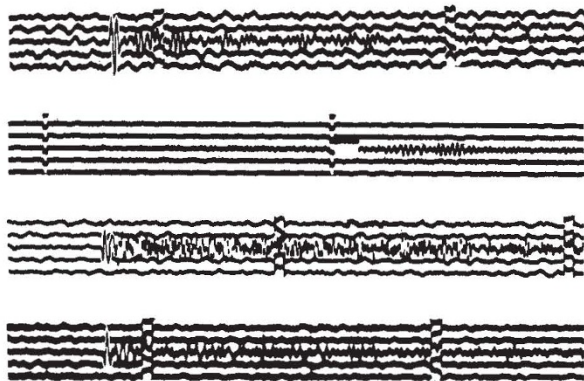


**Fig. 1** Short-period vertical seismograms of earthquake near north-east coast of Greenland on November 26, 1971, of magnitude  $m_b = 5.2$ . Deflexions of trace indicate minute marks; and upward motion of ground is up on records. Station abbreviations, distances and gains are as follows from top to bottom: NUR,  $22.8^\circ$ , 25k; STU,  $32.2^\circ$ , 25k; KBL,  $55.7^\circ$ , 400k; QUE,  $59.6^\circ$ , 200k. The first motion is a clear compression (up) at NUR and a clear dilatational (down) at KBL and QUE. Initiation of P wave and first motion cannot be read at STU, which is inferred to be near a nodal plane. The four stations are labelled on focal mechanism solution in Fig. 2. Arrivals of four P waves are aligned approximately vertically. Light portions of traces are retouched.

These events are characterised by very large areas of perceptibility compared with most shocks of similar magnitudes and energies along plate boundaries. Thus, although they are not numerous, large intraplate shocks constitute an environmental risk that must be taken into account in the design and siting of critical facilities such as nuclear reactors and other large man-made structures. The presence of high compressive stresses in the interiors of many lithospheric plates indicates that the possible triggering of earthquakes by processes that reduce rock strength, such as high-pressure fluid injection and reservoir impounding, must be evaluated carefully.

### Large Compressive Stresses

Determinations of stress *in situ*, principally by the overcoring technique, indicate that measured horizontal compressive stresses are much larger than lateral (and even vertical) stresses calculated from the weight of the overburden in Fennoscandia<sup>5</sup>, eastern and central North America<sup>6-8</sup>, the Colorado Plateau<sup>8-10</sup> and various parts of the USSR<sup>11,12</sup>. Thus, the horizontal component of the stress in these areas must be largely tectonic. Although most of these measurements were made primarily for engineering purposes, Voight<sup>7</sup> recognised that the data may provide important constraints for models of the driving mechanism of large-scale tectonic processes. Nevertheless, very few authors have distinguished between measurements made in what are now recognised as the interiors of plates with those that are pertinent to plate margins.

Sbar and Sykes<sup>8</sup> examined the directions of principal stresses in central and eastern North America as inferred from *in situ* measurements by the overcoring and hydrofracturing techniques, focal mechanisms, and postglacial geological features. They found good agreement among the various techniques and showed that the greatest principal stress trends nearly ENE throughout a large region that includes much of the eastern and central United States. Focal mechanisms of about ten earthquakes in western Europe north of the Alps are characterised by either thrust or strike-slip faulting such that the axes of maximum compressive stress trend consistently north-west<sup>13</sup>. Thus, in two areas where relatively dense observations of stress are available, the maximum compressive stress seems to be horizontal, to be large, and to have a similar trend throughout a broad region. These factors led us to examine the state of stress within lithospheric plates on a global basis.

### Focal Mechanism Data

We examined a magnetic tape file of epicentral locations reported by the National Oceanographic and Atmospheric Administration from 1961 to 1971 for obvious intraplate earthquakes. About half of the seventy-nine mechanism solutions used in this article were determined by us. A list of these events and their mechanism parameters is available from us.

Even though intraplate earthquakes are relatively rare, we were able to obtain a large number of solutions by successfully analysing the first motion of compressional waves for events as small as magnitude  $m_b = 5.0$  using standard short-period records. Clear, impulsive first motions of P (Fig. 1) and PKP are often observed on short-period records for intraplate events of  $5.0 \leq m_b \leq 5.5$ . As many intraplate earthquakes involve dip-slip faulting, stations at distances greater than about  $40^\circ$  (Fig. 2) are often remote from a nodal plane, and therefore record P waves with a distinct first motion. The focal mechanism solution shown in Fig. 2 for an event of  $m_b = 5.2$  represents about the average quality of the various solutions reported here.

These factors and the simplicity of the waveform of P indicate that the corner frequency for these events is higher than about 1 Hz and that the instruments "see" a point source rather than the initiation of motion from a complex moving source as is generally the case for  $m_b > 5.5$ . Most intraplate earthquakes have a larger short-period magnitude,  $m_b$ , than do events along plate boundaries of the same long-period magnitude,  $M_s$ . The enrichment in short-period energy may be caused by greater effective stresses that may be present within plates and/or higher Q paths through the upper mantle, as intraplate events tend to be located in older (and presumably colder and thicker) lithosphere than events along zones of sea-floor spreading and transform faulting.

### Stress Distribution

Figure 3 summarises information on the state of stress as inferred from about eighty focal mechanism solutions of intra-

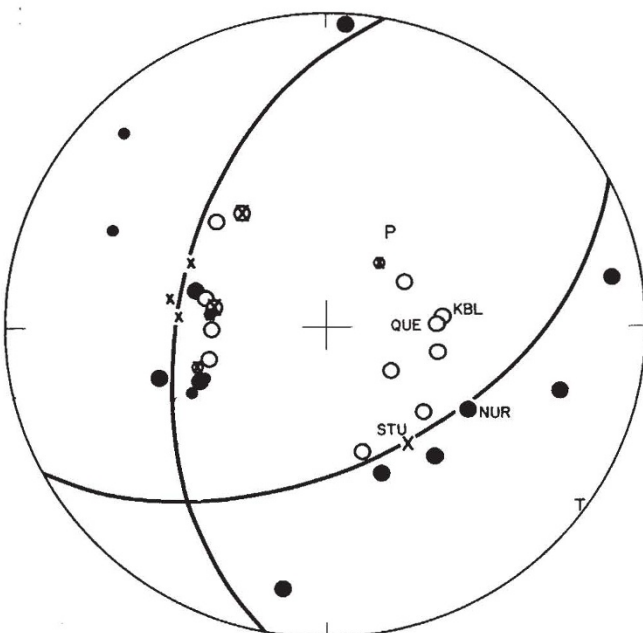


**Fig. 2** Focal mechanism (first motion) solution for earthquake near NE coast of Greenland on November 26, 1971. Plot is equal-area projection on lower hemisphere of radiation field. ●, Compressions; ○, dilatations; X, arrivals near nodal plane; P and T are inferred axes of maximum and minimum compressive stress. Large symbols denote more reliable readings. Solution is characterised by a predominance of normal faulting. First motions shown in Fig. 1 are labelled with three-letter codes for stations.

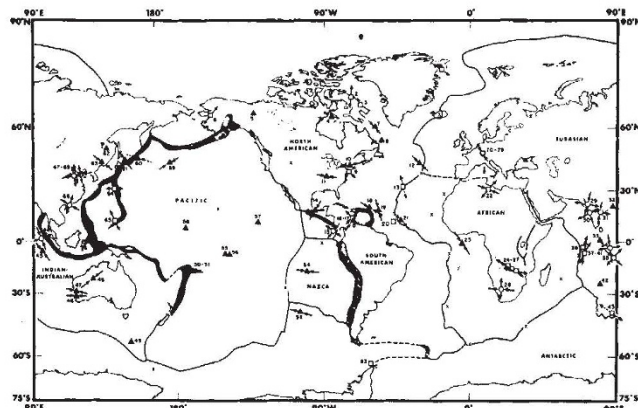


Fig. 3 Worldwide summary of focal mechanism solutions of intraplate earthquakes. ▲, Thrust; ○, strike-slip; □, normal; X, mantle plumes inferred by Morgan<sup>35,36</sup>. Inwardly directed arrows indicate axis of maximum compressive stress (P axis) and outwardly directed arrows denote least compressive stress (T axis). Dashed arrows indicate less reliable directions. Solution in western Europe is representative of ten mechanisms with similar orientation of P axes. Major plates are labelled. Hatching indicates major subduction zones (Mediterranean-Himalayan zone omitted), and solid line represents plate boundaries of extensional and transform type.

plate earthquakes. The solutions are classified as a predominance of either thrust, strike-slip or normal faulting. The first motions of P and PKP are good enough to support this classification for nearly all the events reported. As in other mechanism studies, we equate the P and T axes of the focal solutions with the axes of maximum and minimum compressive stress. For some of the dip-slip events the azimuths of the nodal planes and of the horizontal principal stress are less reliable. Thus, for these events we show only the type of faulting and not the azimuth of the horizontal principal stress. Although the radiation patterns of surface waves can be used to determine this azimuth with greater precision<sup>14-16</sup>, we did not employ it here as substantial additional data analysis is involved.

**Table 1** Number of Focal Mechanism Solutions as a Function of Predominant Fault Type

	Thrust	Normal	Strike-slip
Total events (1 to 69, Fig. 3)	34	22	13
Total minus regions behind arcs	31	18	8
Total minus regions behind arcs, close to ridges or in East Africa	29	4	7 (6 in Indian plate)

In the Pacific plate each of the solutions in Fig. 3 is characterised by thrust faulting. In the Atlantic, the solutions for earthquakes located well away from the mid-Atlantic ridge also involve thrusting. Table 1 indicates that thirty-four (49%) of the total solutions in Fig. 3 involve thrusting. The percentage of thrusting increases to 73% when events located near ridges, behind subduction zones or in East Africa are deleted.

Each of the three main types of faulting is found behind active subduction zones, although a single stress pattern usually prevails behind a given arc. For example, focal solutions and other geophysical data indicate horizontal compression in the lithosphere behind the Honshu and South American arcs and extension behind the Bonin-Mariana and Tonga-Kermadec arcs<sup>17-21</sup>. The state of stress behind active subduction zones does not seem to be typical of that in horizontal portions of the lithosphere. Evidence for extension in the Basin and Range province of the western United States is omitted from Fig. 3 as the tectonics of that region does not seem to be intraplate and it may reflect processes associated with a former subduction zone or the cessation of subduction near the west coast of the United States<sup>22,23</sup>.

Figure 4 shows the type of faulting in oceanic areas as a function of the age of the crust inferred from magnetic anomalies and deep-sea drilling. Thrusting predominates for crust older than 20 m.y.; normal faulting is typical of zones of seafloor spreading at ridge crests and of crust younger than about 10 to 20 m.y. Clearly, the state of stress within the plate has changed from horizontal extension to horizontal compression within the past few tens of millions of years, as it moved away from the ridge crest. The precise age and nature of the boundary between thrusting and normal faulting, however, are not well defined. Six of the eight examples of normal faulting for regions younger than 20 m.y. and not located on ridge crests come from nearly the same location in the Indian Ocean near a large seamount at the southern end of the Chagos-Laccadive ridge<sup>24</sup>. Although solutions characterised by normal faulting were not found near the East Pacific Rise, the one thrusting solution at 10 m.y. indicates that the transition to normal faulting on that ridge system occurs for crust of younger age.

No examples of normal faulting were found for oceanic crust older than 10 to 20 m.y. Normal faulting was detected for an event in New Jersey and for shocks near the coasts of Greenland, the Antarctic Peninsula, and Baffin Island (Fig. 3). All of these events, however, were located on the continental shelf or within continents and not on oceanic crust. We refrain from further speculation about stresses near continental margins, as the number of events is small.

Although not as clear as in the older oceanic lithosphere, many continental areas, interior to plates, are also characterised by large horizontal compressive stresses. Focal mechanism solutions in Fig. 3 and/or measurements of *in situ* stress corroborate this for western Europe and Fennoscandia<sup>5,13</sup>, large areas of the USSR<sup>11,12</sup>, most of the United States east of the Basin and Range Province<sup>8</sup>, western Australia, and peninsular India.

Several examples of normal faulting are found in East Africa (Fig. 3). These events were not located along what are normally regarded as active rifts<sup>27</sup>. Nevertheless, it is difficult to tell if these solutions are better characterised as intraplate events or as earthquakes associated with a wide and complex plate boundary within a continent. A similar problem was encountered in characterising earthquakes in the broad seismic zone, which probably involves continental collision, in the Mediterranean, Central Asia and the Himalayas<sup>26</sup>. The mechanism of the Libyan earthquake in Fig. 3 may be related to this broad plate boundary.

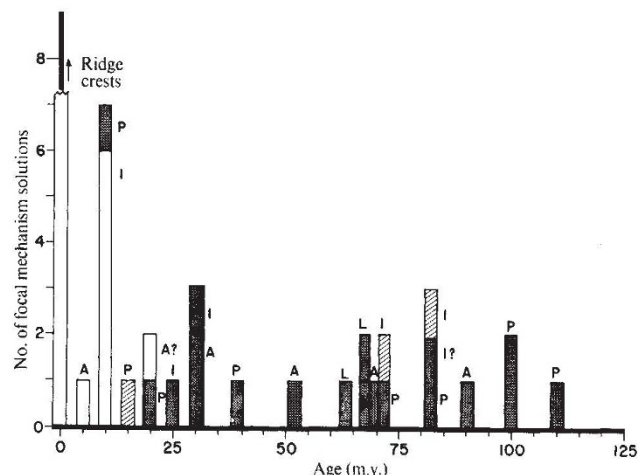


Fig. 4 Type of focal mechanism as a function of age of oceanic crust. Note predominance of normal faulting on, or close to, ridge crests and predominance of thrust faulting for ages greater than 20 m.y. □, Normal; ■■■, thrust; ▨▨▨, strike-slip type faulting. A, Mid-Atlantic ridge; P, Pacific ridges; L, mid-Atlantic ridge; I, mid-Indian ridges.

## Driving Mechanism

From a compilation of focal mechanism solutions Fitch *et al.*<sup>14</sup> concluded that the orientation of the maximum compressive stress (P axis) varied smoothly throughout the Indian-Australian plate. As the axes of least compression (T axes) for their solutions pointed toward the Java trench, they concluded that gravitational sinking of a lithospheric slab at the subduction zone was an important force driving this plate. All of their solutions in the north-east Indian Ocean, however, involved strike-slip faulting. Additional mechanism solutions for this plate (Fig. 3) indicate thrust as well as strike-slip faulting. The two types of solutions show a similar orientation of the maximum compressive stress for nearby events 44 and 45. An explanation of these data is that the minimum and intermediate principal stresses are of similar size, making possible either thrust or strike-slip faulting. As either one of the minimum and intermediate principal stresses is vertical, they both must be similar in magnitude to the stress resulting from the weight of the overburden. This implies that a significant horizontal tensional component is not being applied to the stress field in this region as a result of gravitational sinking. Instead, the mechanism solutions indicate a large horizontal compressive stress, apparently of tectonic origin.

These conclusions are further supported by thrusting mechanisms (Fig. 3) of shocks located seaward of the Aleutian, Kurile, Tonga and Lesser Antillean arcs. If gravitational sinking were primarily responsible for the stress distribution in plates, normal rather than thrust faulting would be typical of intraplate deformation (Fig. 5a). Earthquakes beneath deep-sea trenches<sup>1,21,28-30</sup> are typified by normal faulting, but the causative stress seems to be related mainly to the flexure of the lithosphere<sup>1</sup>. Normal faulting reported for an event on the outer wall of the Japan trench also seems to be related to flexure rather than to a gravitational sinking mechanism as proposed by Shimazaki<sup>31</sup>. Evidence from topographic and gravity anomalies also indicates great horizontal compressive stresses seaward of several Pacific trenches<sup>32,33</sup>. The opening of the South Atlantic is also difficult to explain solely by gravitational sinking as the African and Americas plates are not being subducted except in very local areas<sup>34</sup>. These observations, of course, do not rule out gravitational sinking as a contributory driving force even if it is not the primary driving mechanism. It may well be responsible for the distribution of stress in downgoing plates in island arcs<sup>2</sup>.

Several events in Fig. 3 are located so close to plate boundaries that it is not certain if their mechanisms reflect intraplate stresses or boundary effects. Even though events 50, 51 and 60 are located just seaward of deep-sea trenches, their thrusting mechanisms are distinctly different from normal faulting that

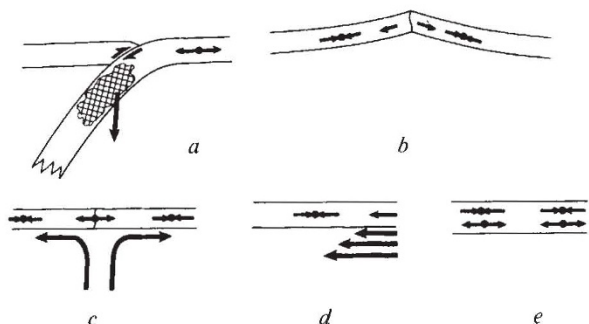


Fig. 5 Schematic diagrams of various mechanisms for generating stresses within lithospheric plates. Single arrows denote relative motions and double arrows denote either compressional (inward) or tensional (outward) deviatoric stresses. *a*, Gravitational sinking in island arc; *b*, gravitational sliding or pushing from ridge; *c*, mantle plume; *d*, rapid flow in asthenosphere; *e*, stresses related to cooling of lithosphere. Hatching in *a* denotes mass excess caused by either cooler material or increased elevation of phase boundaries in sinking slab.

characterises events within trenches. As thrusting is also found elsewhere in the Pacific plate, we interpret these three solutions as intraplate events and not as boundary effects. Events 61, 64 and 65, however, are located behind subduction zones near volcanic arcs. Their mechanisms may be related to the flexure of the lithosphere, other boundary effects, or, in the case of events 64 and 65, to inter-arc spreading<sup>20</sup>. Event 13 was located about 50 km west of the rift valley and the main seismic zone of the mid-Atlantic ridge<sup>25</sup>. It is difficult to characterise this event as a plate boundary or an intraplate phenomenon.

Several other mechanisms for driving plates and for stressing their interiors are shown schematically in Fig. 5. Observations of normal faulting close to active ridges and thrusting at greater distances are compatible with plates being driven from below by flow in the asthenosphere or by gravitational sliding or pushing from the general area of ridge crests. The easterly trends of the maximum compressive stress in the south-east Pacific provide evidence for these two mechanisms, as they are nearly perpendicular to the crest of the East Pacific Rise. The trends for solutions 18, 19, 21, and 23 in the Atlantic, however, are nearly parallel to the axis of the mid-Atlantic ridge. Although the trends for these three solutions are not precisely constrained by first-motion data, the uncertainty probably does not exceed 25° for events 19 and 23. Likewise, the maximum compressive stress for events in western Australia, at least one of which is well constrained to be nearly east-west from the radiation pattern of surface waves and from observations of surface faulting<sup>14</sup>, is nearly parallel to the axis of the nearby branch of the mid-Indian Ocean ridge. Thus, several solutions do not fit a simple model in which gravitational sliding or pushing from a line source located at the ridge crest is the primary motive force of plate tectonics.

Another possible source of compressive stresses within plates is not related to the driving mechanism, but merely to the gradual cooling and thickening of lithospheric plates (Fig. 5) in that stresses may be frozen in as in the cooling of glass. In oceanic areas the transition from normal to thrust faulting occurs for crust about 10 to 20 m.y. old. This age is nearly the same as the thermal time constant for the formation and destruction of the lithosphere<sup>1,34</sup>. Nevertheless, we would expect that compressive stresses frozen into the oceanic lithosphere by this mechanism would exhibit some systematic alignment with respect to the direction of lithospheric cooling and thickening. As in the case of gravitational sliding, the P axes of focal mechanisms do not seem to have such a systematic orientation. Near solutions 18, 19 and 23, however, the pattern of sea-floor evolution is not well known and we cannot evaluate this mechanism definitively.

Morgan<sup>35,36</sup> suggests that mantle plumes are the main driving mechanism of plates. We attempted to test the simple case where each of the plumes he proposes (Fig. 3, X) was of equal strength and the maximum compressive stress was orientated radially about each plume. The orientations of the P axes from focal mechanisms do not obviously correlate with those predicted by the simple model. Also, the directions of principal stresses in Fig. 3 do not seem to correlate with directions of absolute plate motions inferred by Morgan<sup>35,36</sup> from tracks of hot spots.

Although we cannot isolate a single mechanism as the driving force of plate tectonics, data on the distribution of stress on a worldwide basis provide valuable constraints on proposed mechanisms. We refrain from looking for patterns in the directions of principal stresses in Fig. 3 as the data points are widely spaced except for those in eastern North America and northern Europe where the stress fields do, in fact, appear to be uniform over large areas. Additional focal mechanism solutions and *in situ* stress measurements by the overcoring and hydrofracturing techniques should help to clarify if stress fields generally vary rapidly or are nearly uniform in extent over broad areas in the interiors of most plates. The density of stress determinations in oceanic areas could be greatly

increased by using ocean-bottom seismographs for first-motion studies and by making hydrofracturing measurements in holes drilled into layer 2 of the oceanic crust.

This work was supported by the National Science Foundation, the US Geological Survey and the Advanced Research Projects Agency of the Department of Defense through the Air Force Cambridge Research Laboratories. We thank Paul Pomeroy and Walter Pitman for reviewing the manuscript and D. McKenzie for discussions.

Received July 7; revised August 6, 1973.

- <sup>1</sup> Isacks, B. L., Oliver, J., and Sykes, L. R., *J. geophys. Res.*, **73**, 5855 (1968).
- <sup>2</sup> Isacks, B., and Molnar, P., *Rev. geophys. Space Phys.*, **9**, 103 (1971).
- <sup>3</sup> McKenzie, D., and Parker, R. L., *Nature*, **216**, 1276 (1967).
- <sup>4</sup> Smith, W. E. T., *Dom. Obs. Pamph.*, **26**, 271 (1962).
- <sup>5</sup> Hast, N., *Tectonophysics*, **8**, 169 (1969).
- <sup>6</sup> Hooker, V. E., and Johnson, C. F., in *Proc. Fourth Rock Mech. Symp.* (Department of Energy, Mines and Resources, Ottawa, Canada, 1967).
- <sup>7</sup> Voight, B., *Am. Assoc. Petrol. Geol. Mem.*, **12**, 955 (1969).
- <sup>8</sup> Sbar, M. L., and Sykes, L. R., *Bull. geol. Soc. Am.*, **84**, 1861 (1973).
- <sup>9</sup> Raleigh, C. B., Healey, J. H., and Bredehoef, J. D., *Geophys. Monog.*, **16**, 275 (1972).
- <sup>10</sup> Haimson, B. C., in *Proc. Fourteenth Symp. Rock Mech.*, 689 (American Society of Civil Engineers, 1973).
- <sup>11</sup> Kropotkin, P. N., *Phys. Earth planet. Int.*, **6**, 214 (1972).
- <sup>12</sup> Turchanivov, I. A., Markov, G. A., Gzovsky, M. V., Kazikayer, D. M., Frenze, U. K., Batugin, S. A., and Chabdarova, U. I., *Phys. Earth planet. Int.*, **6**, 229 (1972).
- <sup>13</sup> Ahorner, L., *Geol. Rdsch.*, **61**, 915 (1972).
- <sup>14</sup> Fitch, T., Worthington, M. H., and Everingham, I. B., *Earth planet. Sci. Lett.*, **18**, 345 (1973).
- <sup>15</sup> Mendiguren, J. A., *J. geophys. Res.*, **76**, 3861 (1971).
- <sup>16</sup> Forsyth, D., *Nature*, **243**, 78 (1973).
- <sup>17</sup> Ichikawa, M., *Pap. Meteor. Geophys.*, **16**, 104 (1965).
- <sup>18</sup> Ichikawa, M., *Pap. Meteor. Geophys.*, **16**, 201 (1966).
- <sup>19</sup> Isacks, B., *Abstr. Prog. Seismol. Soc. Am. Annual Meeting* (1969).
- <sup>20</sup> Karig, D. E., *J. geophys. Res.*, **76**, 2542 (1971).
- <sup>21</sup> Katsumata, M., and Sykes, L. R., *J. geophys. Res.*, **74**, 5923 (1969).
- <sup>22</sup> Scholz, C., Barazangi, M., and Sbar, M. L., *Bull. geol. Soc. Am.*, **82**, 2979 (1971).
- <sup>23</sup> Smith, R., and Sbar, M. L., *Bull. geol. Soc. Am.* (in the press).
- <sup>24</sup> Heezen, B. C., and Tharp, M., *Indian Ocean Floor* (map) (National Geographic Society, Washington DC, 1967).
- <sup>25</sup> Sykes, L. R., *J. geophys. Res.*, **75**, 6598 (1970).
- <sup>26</sup> Molnar, P., Fitch, T. J., and Wu, F. T., *Earth planet. Sci. Lett.* (in the press).
- <sup>27</sup> Maasha, N., and Molnar, P., *J. geophys. Res.*, **77**, 5731 (1972).
- <sup>28</sup> Stauder, W., *J. geophys. Res.*, **73**, 7693 (1968).
- <sup>29</sup> Johnson, T., and Molnar, P., *J. geophys. Res.*, **77**, 5000 (1972).
- <sup>30</sup> Molnar, P., and Sykes, L. R., *Bull. geol. Soc. Am.*, **80**, 1639 (1969).
- <sup>31</sup> Shimazaki, K., *Phys. Earth planet. Int.*, **6**, 397 (1972).
- <sup>32</sup> Hanks, T. C., *Geophys. J.*, **23**, 173 (1971).
- <sup>33</sup> Watts, A. B., and Talwani, M., *Geophys. J.* (in the press).
- <sup>34</sup> McKenzie, D. P., *Geophys. J.*, **18**, 1 (1969).
- <sup>35</sup> Morgan, W. J., *Bull. Am. Assoc. Petrol. Geol.*, **56**, 203 (1972).
- <sup>36</sup> Morgan, W. J., *Geol. Soc. Am. Mem.*, **132**, 7 (1973).

## LETTERS TO NATURE

### PHYSICAL SCIENCES

#### Infrared and X-ray Variability of Cyg X-3

CYGNUS X-3 is a candidate for the radio source which in September 1972 experienced a series of exceptional radio outbursts<sup>1</sup>. The X-ray emission is chiefly distinguishable as showing periodic intensity variations with a period of 4.8 h (ref. 2); if these variations are caused by an eclipse, the orbital period is the shortest observed up to this time from an X-ray source. The definite identification of the radio source with the X-ray source has remained unconfirmed up to now because of the poor positional accuracy of the X-ray source; the error box in the 3U catalogue is about  $1 \times 2$  arc min (ref. 3). Although there is no visual candidate for Cyg X-3 to a limit of  $\sim 2 \times 10^{-32} \text{ W m}^{-2} \text{ Hz}^{-1}$  ( $V \sim 23$  mag) (ref. 4), at infrared wavelengths Becklin *et al.*<sup>5</sup> found a source coincident to  $\pm 2$  arc s with the radio position. At  $2.2 \mu\text{m}$ , the flux density is approximately  $2 \times 10^{-28} \text{ W m}^{-2} \text{ Hz}^{-1}$ , whereas the 1.65 to  $2.2 \mu\text{m}$  colour of the infrared source is consistent with a Rayleigh-Jeans spectrum which is reddened by 1.5 mag at  $2.2 \mu\text{m}$  by the interstellar medium. There is no reason to suppose that the source is intrinsically more luminous in the infrared than at visible wavelengths.

Here we describe the coordinated X-ray and infrared observations at Cyg X-3. These observations have led to the discovery of a synchronous 4.8-h periodicity in the flux density of the infrared source. This uniquely associates the X ray with the infrared source, and hence, through the positional coincidence, with the radio object. In addition, short term variability in the infrared flux of Cyg X-3 is described which may be related to the flares seen at radio wavelengths. An improved estimate of the X-ray position is also given.

The main infrared observations presented here were made

at the Cassegrain focus of the Hale 200-inch telescope on July 9 and 11, 1973, UT. The photometer, using a focal plane chopper to remove background radiation, has been described by Becklin and Neugebauer<sup>6</sup>; both a PbS and an InSb detector were used at  $2.2 \mu\text{m}$ . The area around Cyg X-3 is crowded, and so a 5 arc s small aperture was used and the photometer oriented to avoid contamination by field stars.

X-ray data were obtained on July 9, 1973, UT, using a collimated proportional counter sensitive in the 1 to 3 Å wavelength range which is part of the MSSL X-ray package on board Copernicus. The system has a field of view of approximately  $3^\circ$  full width at half maximum and an effective area of  $17 \text{ cm}^2$ . The counter background is reduced by an anti-coincidence system between the stellar and calibration sections of the detectors, and by pulse-shape discrimination of the output from the stellar channel. The resulting background rate in orbit is of the order of 30 counts per integration period of approximately 62.5 s and this is removed using correlations derived between the 1 to 3 Å guard channel signal and the background level observed when no X-ray emitting object is within the field of view of the detector. The guard channel outputs the number of pulses registered due to the previously mentioned rejection systems. The Copernicus spacecraft provides a stabilised platform which enables continuous observation of a source to be made for extended periods. Breaks in the X-ray data are caused by Earth occultation and passage through the South Atlantic Anomaly.

Following the initial discovery of the infrared object<sup>5</sup>, refined measurements were obtained on the position and size of the infrared source as well as the presence of other infrared sources in the field. The location of the Cyg X-3 infrared candidate was remeasured with respect to visual local field stars which are also infrared sources; four such objects, whose positions were determined with respect to 23 SAO stars, lie within  $\sim 30$  arc s of Cyg X-3. The 1950.0 positions of the infrared and the radio source are given in Table 1.